Taylor & Francis
Taylor & Francis Group

Synthetic Communications

An International Journal for Rapid Communication of Synthetic Organic Chemistry

ISSN: 0039-7911 (Print) 1532-2432 (Online) Journal homepage: https://www.tandfonline.com/loi/lsyc20

Amide derivatives of 4-azaindole: Design, synthesis, and EGFR targeting anticancer agents

Puli Venkat Swamy, Vukoti Kiran Kumar, Ruddarraju Radhakrishnam Raju, Regalla Venkata Reddy, Anindita Chatterjee, Gangarapu Kiran & Gattu Sridhar

To cite this article: Puli Venkat Swamy, Vukoti Kiran Kumar, Ruddarraju Radhakrishnam Raju, Regalla Venkata Reddy, Anindita Chatterjee, Gangarapu Kiran & Gattu Sridhar (2019): Amide derivatives of 4-azaindole: Design, synthesis, and EGFR targeting anticancer agents, Synthetic Communications, DOI: 10.1080/00397911.2019.1683206

To link to this article: https://doi.org/10.1080/00397911.2019.1683206

SYNTHETIC COMMUNICATIONS®
https://doi.org/10.1080/00397911.2019.1683206

Amide derivatives of 4-azaindole: Design, synthesis, and EGFR targeting anticancer agents

Puli Venkat Swamy[a], Vukoti Kiran Kumar[a], Ruddarraju Radhakrishnam Raju[b], Regalla Venkata Reddy[a], Anindita Chatterjee[a], Gangarapu Kiran[c], and Gattu Sridhar[d]

[a]Department of Chemistry, Koneru Lakshmaiah Education Foundation, Guntur, Andhra Pradesh, India; [b]Dr. MACS Bio-Pharma Pvt. Ltd, Medak Telangana, India; [c]Department of Pharmaceutical Analysis and Chemistry, School of Pharmacy, Anurag Group of Institutions, Medchal, Telangana, India; [d]Organic and Biomolecular Chemistry Division, CSIR-Indian Institute of Chemical Technology, Hyderabad, India

ABSTRACT

A series of amide derivatives of azaindole-oxazoles (**11a–n**) were designed and synthesized and their structures were confirmed by ^{1}HNMR, ^{13}CNMR and mass spectral analysis. Further, these derivatives were screened for their anticancer activity against human cancer cell lines viz; MCF7 (breast), A549 (lung) and A375 (melanoma). *In vitro* anticancer activity screening indicated that most of the hybrids exhibited potent inhibitory activities in a variety of cancer cell lines. Among the compounds **11d, 11e, 11f, 11j, 11k, 11l, 11m,** and **11n** were exhibited more potent activity than standard, in those mainly two compounds **11m** and **11j** were exhibited excellent activity in MCF-7 cell line with IC_{50} values 0.034 and 0.036 μM. Moreover, all these compounds were carried out their molecular docking studies on EGFR receptor results indicated that two potent compounds **11m** and **11j** were strongly binds to protein EGFR (PDB ID: 4hjo). It was found that the energy calculations were in good agreement with the observed IC_{50} values.

GRAPHICAL ABSTRACT

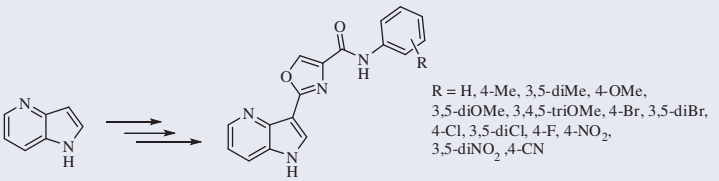

ARTICLE HISTORY
Received 14 July 2019

KEYWORDS
Azaindole; oxazole; docking and anticancer activity

Introduction

Nitrogen-containing heterocyclic compounds play a very important role in medicinal and pharmaceutical chemistry. Indole is a nitrogen-containing fused heterocyclic

CONTACT Puli Venkat Swamy venkatswamichem1@gmail.com Department of Chemistry, Koneru Lakshmaiah Education Foundation, Vaddeswaram, Guntur, Andhra Pradesh, 522502, India.
Color versions of one or more of the figures in the article can be found online at www.tandfonline.com/lsyc.
Supplemental data for this article can be accessed on the publisher's website.

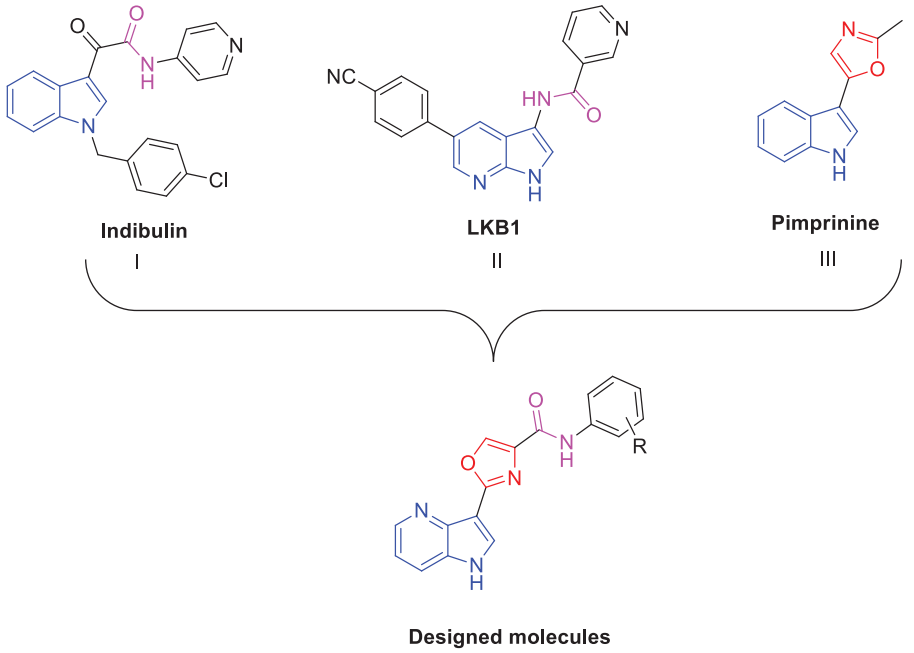

Figure 1. Anticancer target indole molecules (**I** & **II**) and biologically active indole-oxazole molecule (**III**).

compound and widely distributed in many bioactive compounds and natural products[1] such as alkaloids, plant, animal and microbial hormones. Among the based on indole drugs, Indiublin and LKBI showed anticancer activity against various cancer cell lines. Indibulin (**I**, Figure 1) (also called ZIO-301 and D-24851) is a novel synthetic anti-mitotic agent that binds tubulin, destabilizes microtubulin polymerization and arrests tumor cell growth at the G2/M phase. Microtubulins are well-established targets for anti-cancer drug development[2,3] and also Indibulin had been used Phase I/II trials for the treatment of metastatic breast cancer (NCT01113970) and Liver kinase B1 (**II**, Figure 1) (LKB1, also known as STK11) was first identified as the causal mutation in Peutz–Jeghers Syndrome (PJS), a rare inherited autosomal dominant disorder and it was characterized by the development of gentle gastrointestinal hamartomas and the early onset of cancer.[4] However, more than a decade later, LKB1 has become recognized as a critical tumor-suppressor gene that is regularly mutated in a broad spectrum of human cancers. Similarly, 4-azaindoles have generated an increased interest due to their structural similarities with indoles and played key role in medicinal chemistry.[5–7] These were exhibited a variety of biological activities such as antimalarial,[8] anthelmintic,[9] non-narcotic antitussive,[10] anti-diabetic,[11] antiviral,[12] anticholinesterase,[13,14] and anticancer.[15–17]

During the last century, much research has concentrated on the isolation, biological activities and synthesis of indole-oxazole due to their biological and pharmaceutical significance. For example, pimprinine (**III**, Fig. 1) is an indole-alkaloid and demonstrated good monoamine oxidase (MAO) inhibition[18] and antiepileptic[19] activity. In addition, oxazoles are five-member heterocyclic essential structural units for medicinal chemists and have attracted continuing interest over the years. Which are displayed versatile

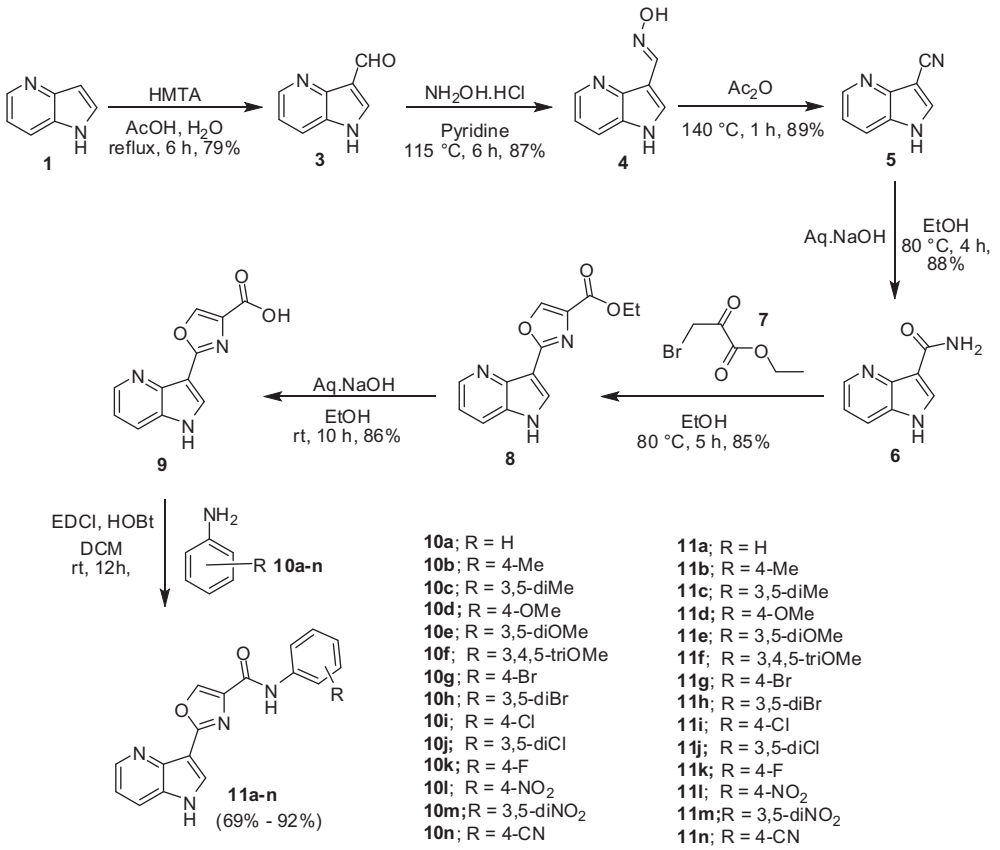

Scheme 1. 4-Azaindole amide derivatives.

biological activities including anticancer,[20] A_{2A} adenosine receptor antagonists,[21] anti-HIV,[22] anti-tuberculotic,[23] antifungal,[24] insecticidal,[25] herbicidal[26] and receptor tyrosine kinases (RTK).[27]

Based on the biological evaluation and mechanism studies of anticancer indoles revealed that these compounds have been showing target diverse pathways in cancer cells. Accordingly, biological importance and current application of indole-derived compounds (**I**, **II,** & **III**) as shown in (Figure 1), we have designed and synthesized novel amide derivatives of azaindole-oxazole as anticancer agents. This manuscript summarizes the versatility of indole-oxazole core structure and SAR studies, arranged by their biological activity, which leads to the discovery of diverse new anticancer agents and subsequently *in silico* molecular docking were evaluated.

Results and discussion

Chemistry

The synthetic route of target compounds (**11a-n**) as shown in Scheme 1. Compound **1** was treated with HMTA in acetic acid and H_2O at reflux for 6 hours to afford pure aldehyde compound **3** in good yield. Next, the carbonyl addition by compound **3** with

Table 1. *In vitro* cytotoxic activity of compounds (**11a–n**) in (IC_{50} μM).

Comp No	R	MCF-7 (breast)	A-549 (Lung)	A375 (Melanoma)
11a	H	3.78 ± 0.31	–	–
11b	4-Me	3.89 ± 0.29	4.34 ± 0.39	9.67 ± 0.91
11c	3,5-diMe	14.39 ± 0.99	7.32 ± 0.66	5.30 ± 0.39
11d	4-OMe	1.11 ± 0.12	0.78 ± 0.065	1.54 ± 0.13
11e	3,5-diOMe	2.40 ± 0.17	1.73 ± 0.14	0.84 ± 0.069
11f	3,4,5-triOMe	0.90 ± 0.11	1.56 ± 0.13	2.67 ± 0.19
11g	4-Br	6.10 ± 0.49	–	–
11h	3,5-diBr	3.76 ± 0.31	0.95 ± 0.083	1.25 ± 0.093
11i	4-Cl	4.89 ± 0.36	8.67 ± 0.71	15.9 ± 1.1
11j	3,5-diCl	0.036 ± 0.0023	0.92 ± 0.081	1.74 ± 0.13
11k	4-F	0.66 ± 0.051	1.33 ± 0.11	–
11l	4-NO_2	0.22 ± 0.019	0.14 ± 0.013	–
11m	3,5-diNO_2	0.034 ± 0.002	0.59 ± 0.044	0.28 ± 0.019
11n	4-CN	1.23 ± 0.093	0.28 ± 0.022	1.77 ± 0.14
Doxorubicin		2.02 ± 0.17	2.18 ± 0.18	5.51 ± 0.039

The results were expressed as the (IC_{50} μM). "–" = Not active.
Values are mean ± SEM.

hydroxylamine hydrochloride in pyridine at 115 °C for 6 hours to afford pure oxime formation compound **4**. Then, nitrile formation by reacted with acetic anhydride at 140 °C for 1 hour to afford pure cyano compound **5** and then followed by partial hydrolysis with aqueous NaOH in ethanol at 80 °C for 4 hours to afford amide compound **6**. This amide intermediate was reacted with ethyl 3-bromo-2-oxopropanoate **7** in ethanol at reflux for 5 hours to give oxazole compound **8.** Afterward, this intermediate **8** undergoes basic hydrolysis with aqueous NaOH in ethanol at room temperature for 10 hours to give acid compound **9**. Finally, this acid **9** was coupled with different substituted aromatic amines (**10a–n)** by using reagents EDCI, HOBt in CH_2Cl_2 at room temperature for 12 hours to afford target compounds (**11a–n**). The structures of the synthesized compounds were confirmed by ^{1}H NMR, ^{13}CNMR and mass spectral data. As a representative example, the ^{1}HNMR spectra of N-(3,5-dinitrophenyl)-2-(1H-pyrrolo[3,2-b]pyridin-3-yl)oxazole-4-carboxamide **(11 m)** is characterized as follows: One broad singlet appears at 9.57 (brs, 1 H) ppm corresponds to amide proton –CON**H**–, one singlet at 9.73 (s, 2 H) corresponds to –Ar**H** and one singlet appear at 9.87 (s, 1 H) corresponds to isoxazole –**H**. ^{13}C NMR spectral data shown singlet peak appear at 145.8 ppm is corresponds to isoxazole –**C**–, singlet at 159.7 ppm corresponds to isoxazole –O–**C**=N and singlet appear at 161.8 ppm corresponds to keto carbon –**C**O–. The mass spectra of the synthesized compounds showed 395 $[M+H]^+$ peaks in agreement with their molecular formula.

Biological evaluation

In vitro cytotoxicity

Newly synthesized compounds (**11a–n**) were tested for their anticancer activity against three human cancer cell lines including breast (MCF7), lung (A549) and melanoma (A375) by MTT assay. Here positive control used as doxorubicin and results are expressed in IC_{50} with μM and incorporated in Table 1 and also shown in bar diagram Figure 2. *In vitro* anticancer activity, screening indicated that most of the hybrids exhibited potent inhibitory activities in a variety of cancer cell lines with low micromolar to

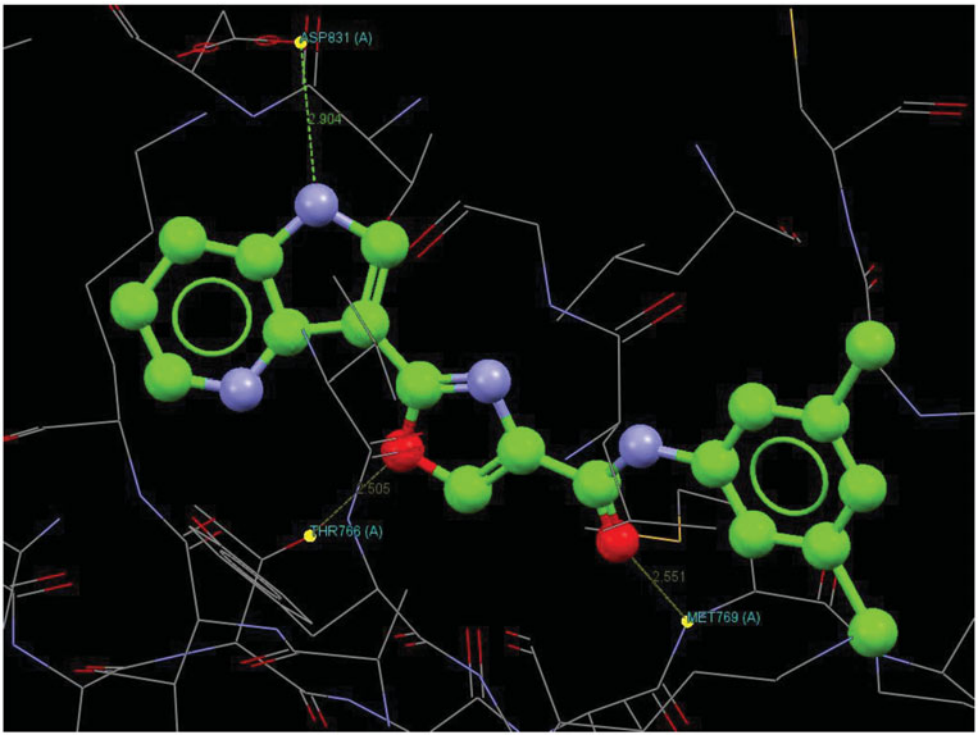

Figure 2. Docking pose of compound **11j** (Ball and stick model) in the EGFR (PDB ID: 4hjo) binding pocket. White line represents the hydrogen bonding. Only the key residues are shown for clarity.

submicromolar IC_{50} values. Among them, compounds **11d, 11e, 11f, 11j, 11k, 11 l, 11 m** and **11n** were exhibited more potent activity than standard. Especially two compounds **11 m** and **11j** were exhibited excellent activity against MCF-7 cell line with IC_{50} values 0.034 and 0.036 μM. In general as compared with the number of cell wises, the highest activity shown by the compounds **11 m** and **11j** were the most active and effective against three cell lines, in which compounds **11 m** ($IC_{50} = 0.034 \pm 0.002$, 0.59 ± 0.044, and 0.28 ± 0.019 μM) and **11j** ($IC_{50} = 0.036 \pm 0.0023$, 0.92 ± 0.081 and 1.74 ± 0.013 μM) for MCF7 (Breast), A549 (Lung) and A375 (Melanoma), respectively. The next better activity showed by compounds **11 l** and **11k** against two cancer cell lines, in which compound **11 l** ($IC_{50} = 0.22 \pm 0.019$ and 0.14 ± 0.013 μM) and **11k** (IC_{50}=0.66 ± 0.051 and 1.33 ± 0.11 μM) for MCF7 (Breast) and A549 (Lung), respectively. The remaining compounds **11d**, **11e**, **11f,** and **11n** also showed good inhibition of three or two cancer cell lines such as breast, lung, and melanoma as shown in Table 1.

The structure-activity relationships (SARs) were established from the anticancer data reported in Table 1. Firstly, the electron-donating analogs (**11a-f**) were described by the most active compound **11d** at the para position of 4-methoxy showed more potent activity.

Further, in this way introduced more methoxy groups at phenyl ring part by tri methoxy analog **11f** at di meta and para positions and compound **11e** at di meta positions results were observed decreasing activity. In that next, simple phenyl analog **11a** and methyl substituted analogs **11b** and **11c** were not active as compared with methoxy analogs (**11d–f**) and also with the standard drug.

Secondly, in the electron with-drawing series (**11g–n**) a dramatic change in activity was observed. The most active analogs such as dinitro **11m** and dichloro **11j** at meta positions of phenyl ring displayed activity in micro molars. In such a way, the next better activity compounds **11l** > **11k** introduced nitro > fluoro at para position displayed loss in the melanoma cell. Consequently, compound **11n** at the para position of cyano resulted in good activity as compared with halogen analogs **11h**, **11i** and **11 g** displayed weaker activities. Finally, in conclusion, most of the with-drawing substitution analogs (**11j–n**) at the phenyl part were found to be the most active of the series. In summary, the information of SAR provided us a guideline to improve the anticancer activity in future structural modification.

Molecular docking studies

The protein receptors EGFR is a striking target in the cancer disease. The epidermal growth factor receptor (EGFR) is the cell-surface receptor for members of the epidermal growth factor family of extracellular protein ligands.[28] It lives on the cell surface and driven by binding of its specific ligands it plays a major role in the ductal development of the mammary glands.[29–31] Overexpression of EGFR associated with a number of cancers, including squamous-cell carcinoma of the breast, lung, anal cancers,[32] glioblastoma and epithelian tumors of the head and neck.[33] These somatic mutations involving EGFR lead to its constant activation, which produces uncontrolled cell division.

In this regard, we have screened all compounds in molecular docking studies and we found interesting idea in the process of exploration of results. In that two molecules **11j** and **11 m** approaches strongly to receptor EGFR protein as showing by their minimum binding energies 68.85 and 68.58 Kcal/mol, respectively. The docking results were found to be in good agreement with *in vitro* experimental IC_{50} values (Table 2). Figures 3 and 4 show the best conformations of **11j** and **11 m** forming a cluster into the binding pocket of EGFR receptor. The GOLD program was used to identify favorable conformations and possible interaction regions at the active site of the EGFR enzyme (4HJO). All the top-ranked conformations of (**11a–n**), were orientated in such a way as to insert themselves

Table 2. Docking interations.

S.No.	Compound	Binding Energy (kcal mol^{-1})	Number of hydrogen bonds	Residues involved in hydrogen bonding
1	**11a**	62.59	3	Asp831(3.06), Met769(2.60), Thr830(2.64)
2	**11b**	64.05	02	Thr766 (2.56), Met769(2.28)
3	**11c**	65.41	03	Asp831(2.91), Thr766(2.59), Met769 (2.59)
4	**11d**	66.52	03	Met769(2.69),Thr830(2.60).Asp831(2.88)
5	**11e**	66.06	02	Met769(3.06), Thr766 (2.97)
6	**11f**	68.20	03	Thr830(2.05), Asp831 (2.96), Lys721(2.72)
7	**11g**	62.75	03	Asp831(2.98), Thr766(2.64), Met769(2.42)
8	**11h**	66.46	03	Asp831(2.99), Thr766 (2.76), Met769(2.47)
9	**11i**	62.82	01	Met769(2.74)
10	**11j**	68.85	3	Thr766(2.50), Asp831(2.90), Met769(2.55)
11	**11k**	60.22	2	Met769(2.54), Thr766(2.57)
12	**11l**	60.23	3	Met769(2.56), Asp831(2.72), Thr830(2.76)
13	**11m**	68.58	3	Met769(2.72), Asp831(2.75), Thr830(2.79)
14	**11n**	62.47	02	Leu764(2.88) Met769(2.86)
15	**AQ4**	71.91	03	Thr766(2.34),Asp831(2.42), Met769(2.57)

into the same pocket of the EGFR structure, and their docked locations on the active site were very close to that occupied by the co-crystallized ligand '**AQ4**'. Figure 5 shows a superimposition of these docking solutions alongside the docking of the ligand '**11j**' that was co-crystallized with EGFR. In an attempt to explain the differences between the docking scores, an analysis of the polar interactions (hydrogen bonds) for the docked ligands on the active site of EGFR structure are summarized in Table 2 (in supplementary material) along with the distances between the donor atoms involved in this interaction by way of ligand–enzyme complexation. Additionally, details were provided of the docking positions for a number of these derivatives (Figures 3–5). Docking positions were captured using the Hermes program.

The compound **11j**, which possesses a chloro substituent, which presented the most stable GOLD score. By contrast, another nitro analog **11m** also presented a stable GOLD score. Figure 3 shows the analog **11j** establishing H-bonds with the Thr766, Asp831, Met769 residues, with distances of 2.50, 2.90 and 2.55 Å, respectively.

Likewise, Figure 3 demonstrates that Asp831 is involved in H-bond, the nitrogen group of azaindole ring, Thr766 forms H-bond with oxygen group of oxazole and Met 769 with oxygen group of amide. While Figure 4 shows that the **11 m** derivative forms H-bonds with Met769, Asp831, and Thr830 of 2.72, 2.75, and 2.79 Å in length, respectively.

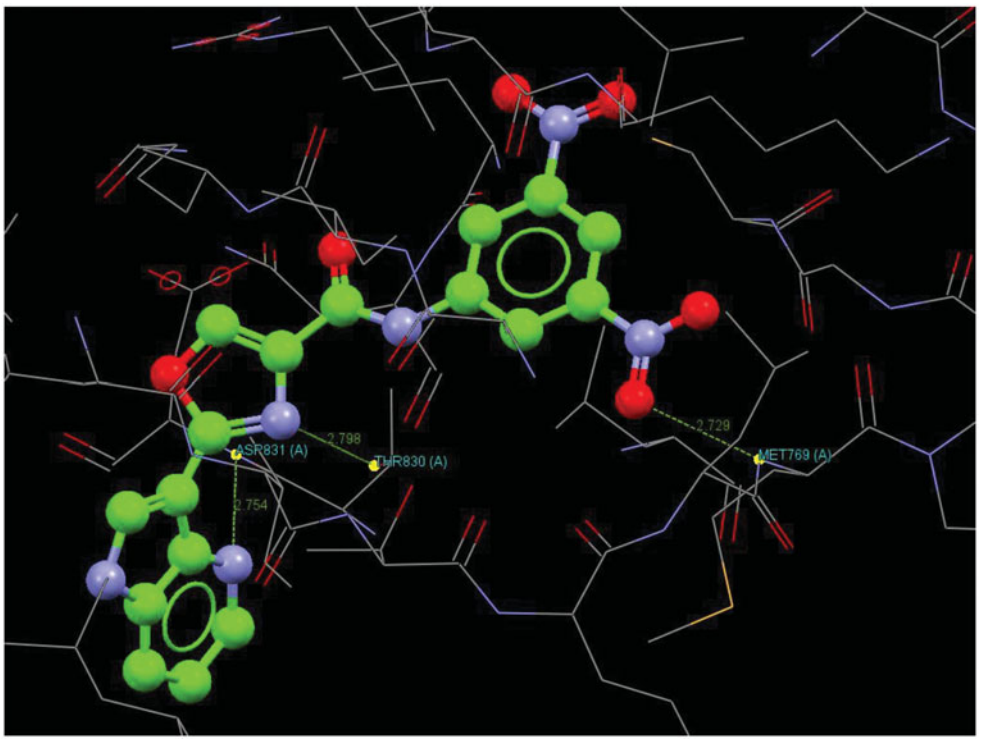

Figure 3. Docking pose of compound **11 m** (Ball and stick model) in the EGFR (PDB ID: 4hjo) binding pocket. White line represents the hydrogen bonding. Only the key residues are shown for clarity.

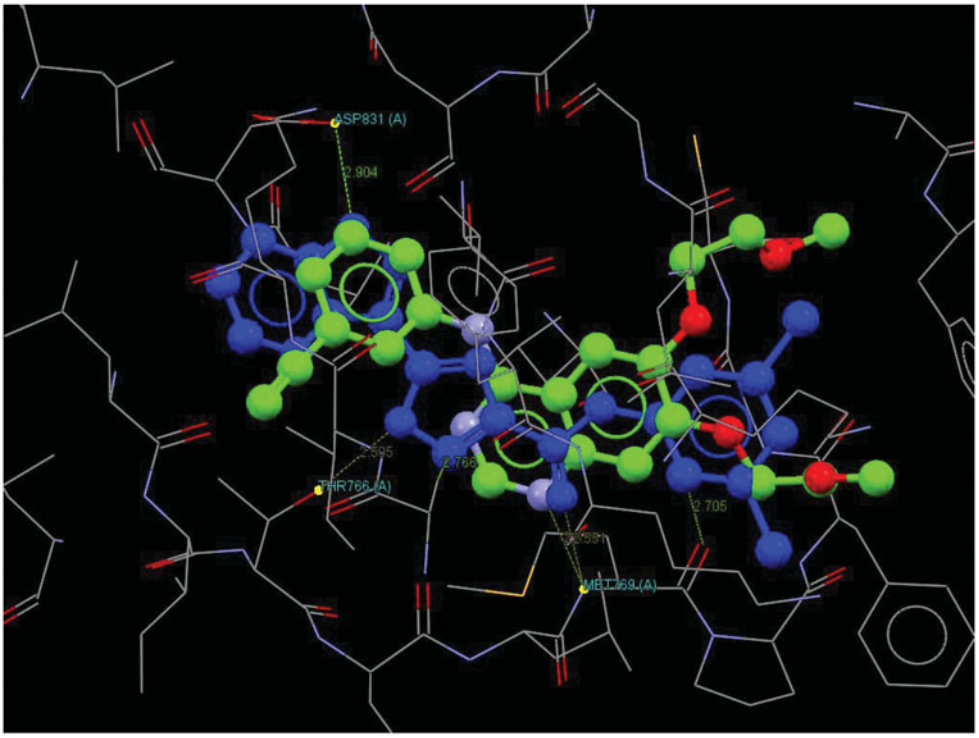

Figure 4. Docked pose of compounds **11j** (Blue, ball and stick) and alongside the cocrystallized ligand '**AQ4**' (yellow, ball and stick model) in the EGFR binding pocket.

Likewise, Figure 4 demonstrates that Asp831 is involved in the H-bond with the nitrogen group of azaindole ring, Met769 forms H-bond with nitro group on benzene and Thr830 with nitro group of oxazole.

All these derivatives (**11a–n)** have shown constant H-bond interactions with amino acids Met769, Asp831, Thr830. In conclusion, the experimental *in vitro* results strongly correlate with the molecular docking analysis.

Furthermore, the docking has been validated by using Auto dock and the compounds **11j** and **11 m** have shown same interactions with EGFR (4HJO). The compound **11j** has shown (Figure 5) H-bond interaction Met769 and Asp 831 and similarly, **11 m** has shown (Figure 6) H-bond interactions with Met769, Lys721, Arg752, and Thr766.

Drug-likeness and ADME properties

Bioavailability of amide derivatives of 4-azaindole (**11a–n**) was accessed through ADME (Adsorption, Distribution, Metabolism, and Excretion) using molinspiration. In order to explore drug-like properties of compounds (**11a–n)**, the lipophilicity, expressed as the octanol/water partition coefficient and here it is called logP(o/w), as well as other theoretical calculations such as molecular size, the number of hydrogen bond acceptors and donors, TPSA and % ABS: Percentage of absorption as shown in Table 3.

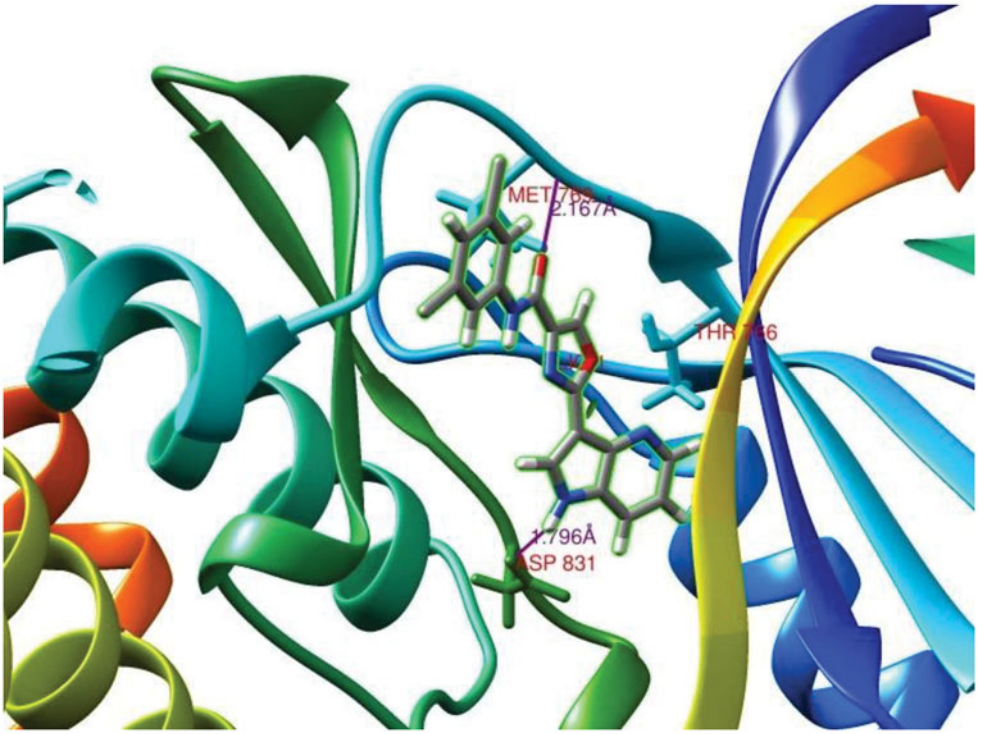

Figure 5. Docking pose of compound **11j** in the EGFR (PDB ID: 4hjo) binding pocket.

The violation of more than one of these rules may indicate problems in the bioavailability of the potential drugs. The results showed all the compounds complied with Lipinski's rule and meet the criteria as shown in Table 3.

Toxicity risk assessment screening

The toxic properties such as mutagenic, tumorigenic, irritant and reproductive effects were screened for the 4-azaindole amide derivatives (**11a–n**) using Molinsperation server. The server is inbuilt with list of about 5300 distinct substructure fragments created by 15,000 commercially available fragments with reported drug score and drug-likeness. Drug score is associated with clogP, drug likeness and toxicity risks as a total value may be used to judge the overall potential to qualify it as a drug. The toxicity screening of all compounds (**11a–n)** showed that no risk of mutagenic, tumorigenic, irritant and reproductive toxicity as shown in Table 4.

Experimental section

All chemicals and reagents were obtained from Aldrich (Sigma–Aldrich, St. Louis, MO, USA), Lancaster (Alfa Aesar, Johnson Matthey Company, Ward Hill, MA, USA) and were used without further purification. Reactions were monitored by TLC, performed on silica gel glass plates containing 60 F-254, and visualization on TLC was achieved by UV light or iodine indicator. ^{1}H and ^{13}C NMR spectra were recorded on Bruker,

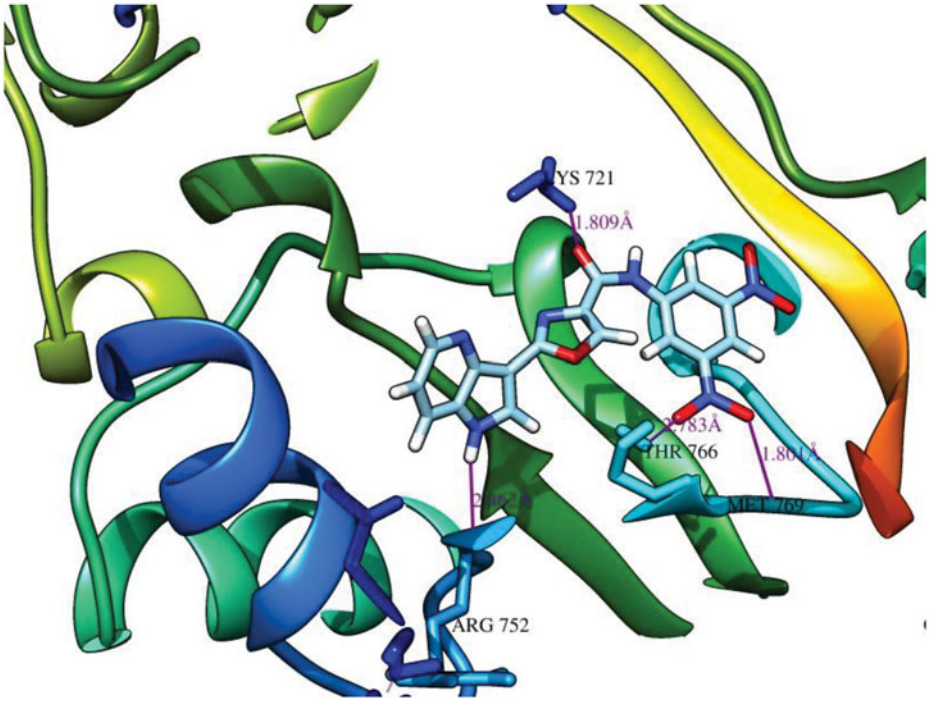

Figure 6. Docking pose of compound **11 m** in the EGFR (PDB ID: 4hjo) binding pocket.

Table 3. ADME properties.

Compound Rule	logP(o/w)<5	MW<500	TPSA<140	HBA<10	HBD<5	nRotB<10	Volume
11a	2.53	304.09	83.81	6	2	3	260.48
11b	2.97	318.34	83.81	6	2	3	277.06
11c	3.35	332.36	83.81	6	2	3	293.60
11d	2.58	334.33	93.05	7	2	4	286.02
11e	2.57	364.36	102.28	8	2	5	311.57
11f	2.16	394.39	111.52	9	2	6	337.12
11g	3.33	383.20	83.81	6	2	3	278.37
11h	4.07	462.10	83.81	6	2	3	296.25
11i	3.20	338.75	83.81	6	2	3	274.01
11j	3.81	373.20	83.81	6	2	3	287.55
11k	2.69	322.30	83.81	6	2	3	265.41
11l	2.48	349.31	129.64	9	2	4	283.8
11m	2.37	394.30	175.46	12	2	5	307.15
11n	2.28	329.32	107.61	7	2	3	277.34

Bruker UXNMR/XWIN-NMR (400 MHz, 300 MHz) instrument. Chemical shifts (δ) are reported in ppm downfield from internal TMS standard. ESI spectra were recorded on Micro mass, Quattro LC using ESI + software with capillary voltage 3.98 kV and ESI mode positive ion trap detector. Melting points were determined with an electrothermal melting point apparatus and are uncorrected.

General procedure for the synthesis of compounds (11a–n):

All the final reactions (**11a–n)** were performed by 200 mg scale. To a stirred solution of acid compound **9** (1.0 equiv) and substituted aromatic amines (**10a–n**) (1.0 equiv) in

Table 4. Toxicity risk assessment of compounds (**11a–n**).

Compound	cLogP	Solubility	Drug likeness	Drugscore	Mutagenic	Tumorigenic	Irritant	Reproductive effect
11a	2.24	−4.37	1.13	0.67	No	No	No	No
11b	2.58	−4.71	1.46	0.65	No	No	No	No
11c	2.93	−5.06	−1.57	0.39	No	No	No	No
11d	2.17	−4.39	1.69	0.69	No	No	No	No
11e	2.1	−4.41	−6.44	0.37	Medium	Medium	No	No
11f	2.03	−4.42	4.33	0.71	Medium	Medium	No	No
11g	2.93	−5.2	0.89	0.32	Medium	Medium	No	No
11h	3.69	−6.04	−2.94	0.24	Medium	Medium	No	No
11i	2.84	−5.11	3.75	0.65	Medium	Medium	No	No
11j	3.45	−5.84	−1.08	0.34	Medium	Medium	No	No
11k	2.34	−4.68	1.64	0.66	No	No	No	No
11l	1.32	−4.83	−12.5	0.35	No	No	No	No
11m	0.39	−5.29	−7.86	0.32	No	No	No	No
11n	2.07	−5.14	−3.84	0.34	No	No	No	No

dichloromethane was added EDCI (1.0 equiv), HOBt (1.0 equiv) and DIPEA (1.2 equiv) at room temperature. The reaction mixture was stirred for 12 h. After completion of the reaction as monitored by TLC, the reaction mixture was diluted with dichloromethane, washed with saturated solution of $NaHCO_3$, dried over anhydrous Na_2SO_4, filtered and concentrated. The crude products were purified by column chromatography eluted with ethyl acetate/hexane to afford the pure compounds (**11a–n**).

N-Phenyl-2-(1H-pyrrolo[3,2-b]pyridin-3-yl)oxazole-4-carboxamide (11a)

The general procedure **11a–n** was followed for the synthesis of **11a**, 211.3 mg in 80% yield. Mp:196–198 °C, ^{1}H NMR (400 MHz, DMSO-d_6): δ 7.30–7.41 (m, 4H), 7.48–7.52 (m, 2H), 7.71 (d, 2H, $J = 7.23$ Hz), 8.89 (d, 1H, $J = 8.19$ Hz), 9.24 (s, 1H), 9.56 (brs, 1H), 9.86 (s, 1H); ^{13}C NMR (75 MHz, DMSO-d_6): δ 97.4, 116.4, 118.6, 122.4, 124.5, 124.9, 131.4, 138.4, 138.9, 139.3, 141.2, 144.8, 145.8, 158.3, 159.8; HRMS (ESI): *m/z* calculated for $C_{17}H_{12}N_4O_2Na$ $[M + Na]^+$ 327.0858, found 327.0851.

Anticancer assay

MTT protocol

The cytotoxic activity of the compounds was determined using the MTT assay. 1×10^4 cells/well were seeded in 200 mL DMEM, supplemented with 10% FBS in each well of 96-well microculture plates and incubated for 24 hours at 37 °C in a CO_2 incubator. Compounds, diluted to the desired concentrations in culture medium, were added to the wells with respective vehicle control. After 48 hours of incubation, 10 mL MTT (3-(4,5-dimethylthiazol-2-yl)-2,5-diphenyl tetrazolium bromide) (5 mg/mL) was added to each well and the plates were further incubated for 4 hours. Then the supernatant from each well was carefully removed, formazon crystals were dissolved in 100 mL of DMSO and absorbance at 540 nm wavelength was recorded.

Docking assay

Molecular docking protocol

Gold 5.6 tool was employed for the *in silico* docking studies to explore the binding mode of ligands and were docked into cavity EGFR (PDB ID: 4HJO). The binding profile for azaindole-oxazole amide derivatives **(11a–n)** ligands with 4HJO was determined and for each ligand ten conformations were generated. The conformations which are having highest ranking were used for further analysis and Gold fitness calculated using Gold docking function.

Conclusion

In conclusion, we have designed and synthesized a novel series of amide derivatives of azaindole oxazoles (**11a–n**) and were evaluated anticancer activity against three human cancer cell lines. Most of the compounds showed moderate to excellent anticancer activity, in those eight analogs **11d, 11e, 11f, 11j, 11k, 11l, 11m,** and **11n** were showed more potent activity than compared with reference drug. The highest activities were found for compounds **11m** and **11j** with IC_{50} values of 0.034 and 00.36 μM in MCF7cell, respectively. Moreover, compound **11m** and **11j** proved to be 58 to 60-folds more active in MCF7 cell as compared with standard. Moreover, molecular docking studies on EGFR receptor results indicated that two compounds **11m** and **11j** of binding interactions strongly correlated with *in vitro* anticancer activity. Further changes and structural modifications of these analogs in order to raise their potency is currently in progress.

Full experimental details, spectral data of the products, ^{1}H NMR and ^{13}C NMR of all the new compounds can be found via the Supplementary Content section of this article's Web page.

Acknowledgments

We would like to express our gratitude and thanks to the Department of Chemistry, Koneru Lakshmaiah University, Guntur for constant encouragement and providing basic research facility.

References

[1] (a) Sundberg, R. J. *The Chemistry of Indoles*. New York, NY: Academic: pp. 113. (b) Lounasmaa, M.; Tolvanen, A. *Nat. Prod. Rep.* **2000**, *17*, 175–191. DOI: 10.1039/a809402k. (c) Hibino, S.; Choshi, T. *Nat. Prod. Rep.* **2001**, *18*, 66–87. DOI: 10.1039/b004055j. (d) Zaimoku, H.; Taniguchi, T.; Ishibashi, H. *Org. Lett* **2012**, *14*, 1656–1658. DOI: 10.1021/ol300280s.

[2] Raab, G.; Komarnitsky, P.; Bacher, G.; Wallner, B.; Kutscher, B. *Am. Assoc. Cancer Res.* **2007**, *67*, 1424.

[3] Wallner, B. P.; Eric Schwartz, B.; Komarnltsky, P. B.; Bacher, G.; Kutscher, B.; Raab, G. Indibulin therapy; Pub. N0.: US 2013/0084345 A1, Pub. Date: Apr. 4, **2013**.

[4] Hemminki, A.; Markie, D.; Tomlinson, I.; Avizienyte, E.; Roth, S.; Loukola, A.; Bignell, G.; Warren, W.; Aminoff, M.; Hoglund, P.; et al. *Nature.* **1998**, *391*, 184–187. DOI: 10.1038/34432.

[5] Fresneda, P. M.; Delgado, S.; Francesch, A.; Manzanares, I.; Cuevas, C.; Molina, P. *J. Med. Chem.* **2006**, *49*, 1217–1221. DOI: 10.1021/jm051090r.
[6] Beswick, P.; Gleave, R.; Swarbrick, M. Patent WO 0,169,241, **2005**.
[7] Tang, P. C.; Sun, L.; McMahon, G. U.S. Patent 6,849,641, **2005**.
[8] Verbiscal, A. J. *J. Med. Chem.* **1972**, *15*, 149–152. DOI: 10.1021/jm00272a008.
[9] Fisher, M. H.; Schwartzkopf, G.; Hoff, D. R. *J. Med. Chem.* **1972**, *15*, 1168–1171. DOI: 10.1021/jm00281a019.
[10] Allegretti, M.; Anacardio, R.; Cesta, M. C.; Curti, R.; Mantovanini, M.; Nano, G.; Topai, A.; Zampella, G. *Org. Process Res. Dev.* **2003**, *7*, 209–213. DOI: 10.1021/op025570t.
[11] Li, Y.-Y.; Wu, H.-S.; Tang, L.; Feng, C.-R.; Yu, J.-H.; Li, Y.; Yang, Y.-S.; Yang, B.; He, Q.-J. *Pharmacol. Res.* **2007**, *56*, 335–343. DOI: 10.1016/j.phrs.2007.08.002.
[12] Abdel-Gawad, H.; Mohamed, H. A.; Dawood, K. M.; Badria, F. A.-R. *Chem. Pharm. Bull.* **2010**, *58*, 1529–1531. DOI: 10.1248/cpb.58.1529.
[13] Ghanei-Nasab, S.; Khoobi, M.; Hadizadeh, F.; Marjani, A.; Moradi, A.; Nadri, H.; Emami, S.; Foroumadi, A.; Shafiee, A. *Eur. J. Med. Chem.* **2016**, *121*, 40–46. DOI: 10.1016/j.ejmech.2016.05.014.
[14] Akrami, H.; Mirjalili, B. F.; Khoobi, M.; Nadri, H.; Moradi, A.; Sakhteman, A.; Emami, S.; Foroumadi, A.; Shafiee, A. *Eur. J. Med. Chem.* **2014**, *84*, 375–381. DOI: 10.1016/j.ejmech.2014.01.017.
[15] MacDonough, M. T.; Strecker, T. E.; Hamel, E.; Hall, J. J.; Chaplin, D. J.; Trawick, M. L.; Pinney, K. G. *Bioorg. Med. Chem.* **2013**, *21*, 6831–6843. DOI: 10.1016/j.bmc.2013.07.028.
[16] Akkoç, M. K.; Yüksel, M. Y.; Durmaz, I.; Atalay, R. Ç. *Turk. J. Chem.* **2012**, *36*, 515–525.
[17] Kumar, D.; Kumar, N. M.; Noel, B.; Shah, K. *Eur. J. Med. Chem.* **2012**, *55*, 432–438. DOI: 10.1016/j.ejmech.2012.06.047.
[18] Takeuchi, T.; Ogawa, K.; Iinuma, H.; Suda, H.; Ukita, K.; Nagatsu, T.; Kato, M.; Umezawa, H.; Tanabe, O. J. *J. Antibiot.* **1973**, *26*, 162–167. DOI: 10.7164/antibiotics.26.162.
[19] Narasimhan, M. J.; Ganla, V. G. *Hindustan Antibiot. Bull.* **1967**, *9*, 138–141.
[20] Freeman, F.; CheN, T.; Van Der Linden, J. B. *Synthesis.* **1997**, *1997*, 861–862. DOI: 10.1055/s-1997-1296.
[21] Holschbach, M. H.; Bier, D.; Stüsgen, S.; Wutz, W.; Sihver, W.; Coenen, H. H.; Olsson, R. A. *Eur. J. Med. Chem.* **2006**, *41*, 7–15. DOI: 10.1016/j.ejmech.2005.07.018.
[22] Ghosh, A. K.; Takayama, J.; Kassekert, L. A.; Ella-Menye, J.-R.; Yashchuk, S.; Agniswamy, J.; Wang, Y.-F.; Aoki, M.; Amano, M.; Weber, I. T.; et al. *Bioorg. Med. Chem. Lett.* **2015**, *25*, 4903–4909. DOI: 10.1016/j.bmcl.2015.05.052.
[23] Li, D.; Gao, N.; Zhu, N.; Lin, Y.; Li, Y.; Chen, M.; You, X.; Lu, Y.; Wan, K.; Jiang, J.-D.; et al. *Bioorg. Med. Chem. Lett.* **2015**, *25*, 5178–5181., DOI: 10.1016/j.bmcl.2015.09.072.
[24] Zhang, M.-Z.; Chen, Q.; Xie, C.-H.; Mulholland, N.; Turner, S.; Irwin, D.; Gu, Y.-C.; Yang, G.-F.; Clough, J. *Eur. J. Med. Chem.* **2015**, *92*, 776–783. DOI: 10.1016/j.ejmech.2015.01.043.
[25] Guo, P.; Huang, J.-H.; Huang, Q.-C.; Qian, X.-H. *Chin. Chem. Lett.* **2013**, *24*, 957–961. DOI: 10.1016/j.cclet.2013.06.033.
[26] Li, G.; Qian, X.; Cui, J.; Huang, Q.; Zhang, R.; Guan, H. *J. Agric. Food Chem.* **2006**, *54*, 125–129. DOI: 10.1021/jf051928j.
[27] Dijkstra, H. P.; Gaulon, C.; Niculescu-Duvaz, D.; Springer, C. J. *Synlett.* **2006**, 1519–1522. DOI: 10.1055/s-2006-941604.
[28] Sebastian, J.; Richards, R. G.; Walker, M. P.; Wiesen, J. F.; Werb, Z.; Derynck, R.; Hom, Y. K.; Cunha, G. R.; DiAugustine, R. P. *Cell Grow. Diff.* **1998**, *9*, 777–785.
[29] McBryan, J.; Howlin, J.; Napoletano, S.; Martin, F. *J. Mammary Gland Biol. Neoplasia.* **2008**, *13*, 159–167. DOI: 10.1007/s10911-008-9075-7.
[30] Sternlicht, M. D.; Sunnarborg, S. W. *J. Mammary Gland Biol. Neoplasia.* **2008**, *13*, 181–196. DOI: 10.1007/s10911-008-9084-6.

[31] Walker, F.; Abramowitz, L.; Benabderrahmane, D.; Duval, X.; Descatoire, V.; Hénin, D.; Lehy, T.; Aparicio, T. *Hum. Path.* **2009**, *40*, 1517–1527. DOI: 10.1016/j.humpath.2009.05.010.

[32] Kumar, V.; Abbas, A.; Aster, J. *Robbins Basic Pathology*. Philadelphia: Elsevier/Saunders, **2013**; pp 179.

[33] Lynch, T. J.; Bell, D. W.; Sordella, R.; Gurubhagavatula, S.; Okimoto, R. A.; Brannigan, B. W.; Harris, P. L.; Haserlat, S. M.; Supko, J. G.; Haluska, F. G.; et al. Activating Mutations in the Epidermal Growth Factor Receptor Underlying Responsiveness of Non–Small-Cell Lung Cancer to Gefitinib. *N. Engl. J. Med.* **2004**, *350*, 2129–2139. DOI: 10.1056/NEJMoa040938.